RAPID COMMUNICATIONS

PHYSICAL REVIEW A VOLUME 58, NUMBER 6 DECEMBER 1998

Single and double ionization of diatomic molecules in strong laser fields

C. Guo, M. Li, J. P. Nibarger, and G. N. Gibson
Department of Physics, University of Connecticut, Storrs, Connecticut 06269

(Received 31 August 1998)

Strong-field single ionization and double ionization of two diatomic molecules, O_2 and N_2, are studied and compared to Xe and Ar, using an intense ultrashort pulse Ti:sapphire laser in the 2×10^{13} to 8×10^{14} W/cm^2 intensity range. N_2 behaves like a structureless atom for both single and double ionization. The recently reported suppression of the $O_2{}^+$ ion yield compared to Xe^+ is confirmed in our experiment, but we show that the suppression is not due to dissociative recombination. Rather, we conclude that the ionization rate of O_2 is below that predicted by tunneling ionization. We extend the study to the double ionization of O_2 and find a distinctly reduced nonsequential double-ionization rate. We find evidence that electronic structure influences strong-field tunneling ionization in molecules.
[S1050-2947(98)50512-4]

PACS number(s): 33.80.Rv, 33.80.Wz, 42.50.Hz

Single-electron ionization of atoms in strong laser fields and related phenomena, such as above-threshold ionization and high harmonic generation, are relatively well understood [1,2]. The properties of double ionization are also well established even if the physical mechanism for nonsequential double ionization (NSDI) still remains unclear [3–5]. Tunneling plays an important role in both single and double strong-field ionization: in the tunneling regime, sequential ionization rates are well described by the Ammosov-Delone-Krainov (ADK) tunneling model [6], and the NSDI rate can be fit by a constant fraction of the first electron tunneling rate [5,7]. The ADK model even predicts threshold intensity into the multiphoton regime [8]. The model is relatively simple: different atoms are only characterized by their ionization potential I_p and the effective quantum numbers, and apparently the details of the electronic structure are unimportant. However, most of the atoms studied intensively with this model are rare-gas atoms, which all have similar closed-shell electronic structures.

Molecules can potentially provide important tests of strong-field dynamics as even easily studied diatomic molecules have a greater diversity of electronic structures. However, the extra degrees of freedom in a molecule could make such studies rather complicated. Fortunately, previous studies have shown that many aspects of strong-field ionization of molecules are similar to those in atoms. For example, in the MPI regime, photoelectron spectroscopy of N_2 showed atomiclike multiphoton resonance similar to Ar as well as details of the electronic structure of $N_2{}^+$ [9]. Several simple molecules have been studied with 10.6-μm CO_2 laser radiation, and the ion yield curves were found to agree with the ADK model [10]. This implies that in the absence of vibrational resonance with the CO_2 laser, ''simple'' molecules are ionized through tunneling as if they were structureless atoms with an ionization potential equal to that of the molecular ground state. More recently, however, with 800-nm Ti:sapphire laser radiation, $O_2{}^+$ was found to have a significantly lower ion yield compared to Xe^+ [11], although Xe has virtually the same single-ionization potential as O_2. This observation led to the hypothesis that while $O_2{}^+$ is produced at the same intensity as Xe^+, the ionized electron can rescatter after one-half cycle of the laser field and recombine with the ion core to form an excited state of O_2 that will dissociate into two neutral oxygen atoms [dissociative recombination (DR)]. The effect of DR would be to reduce the $O_2{}^+$ signal while generating neutral atoms that are not typically measured in such experiments. The anomalous behavior of $O_2{}^+$ was further corroborated using frequency-resolved optical gating techniques with 800-nm and 400-nm radiation [12].

In this paper, we present a comparative study of the single and double ionization of N_2, Ar, O_2, and Xe with 800-nm, ultrashort pulse (30-fs) laser radiation, using both linear polarization (LP) and circular polarization (CP). N_2 and Ar have similar single and double ionization potentials (N_2, 15.58, and 27.12 eV; and Ar, 15.76 and 27.63 eV); O_2 and Xe have nearly the same single ionization potential but somewhat different double ionization potentials (O_2, 12.06 and 24.14 eV; and Xe, 12.13 and 21.21 eV). In comparing N_2 and Ar, we find that N_2 behaves very much like a structureless rare-gas atom in single, double, and nonsequential double ionization. Furthermore, the effects of molecular dissociation are found to be negligible in studying the single ionization behavior. A similar comparison shows the discrepancy in the ion yields between Xe^+ and $O_2{}^+$ for both linear and circular polarization, but we conclude that it does not result from dissociative recombination or any other dissociative processes. Just as in N_2, dissociation appears to be unimportant at this level. We extend the study to the double ionization of O_2 and find that, unlike N_2, ion signals from the metastable and dissociating states of $O_2{}^{2+}$ have different intensity dependences and low NSDI rates. From this we conclude that electronic structure does in fact influence tunneling ionization in molecules at least, and perhaps atoms. The electronic structure effects were not appreciated before probably because only similar closed-shell atoms had been considered.

The laser used to take the data is a Ti:sapphire system running at a 1-kHz repetition rate, producing over 400 μJ/pulse in 30-fs pulses with a center frequency of 800 nm [13,14]. The laser pulses are focused with an on-axis parabolic mirror in a high-vacuum chamber (base pressure $<5\times10^{-10}$ torr). The ions are extracted by a dc field through a

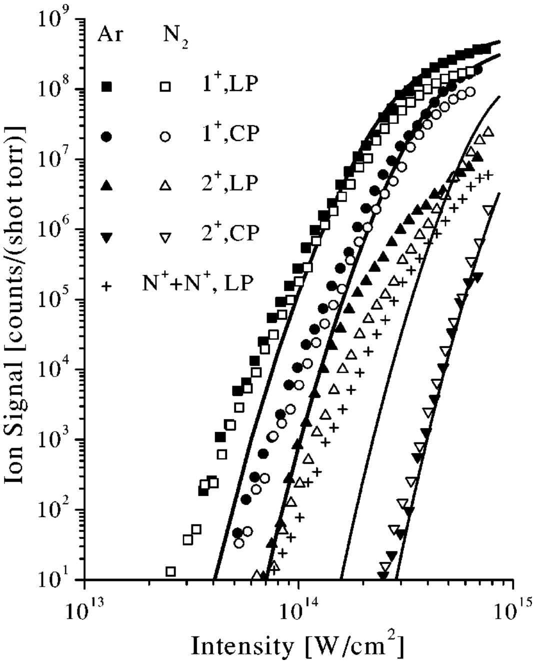

FIG. 1. Single- and double ionization yields for N_2 and Ar using linear polarization (LP) and circular polarization (CP). Calculations based on the ADK model are shown by the full curves. The $N_2{}^+$ data are slightly reduced at the highest intensities due to detector saturation.

1-mm-diam pinhole and are detected with a microchannel plate at the end of a time-of-flight (TOF) mass spectrometer [15]. The signal is further amplified and discriminated so that the ions can be individually counted by a computer. The electron multiplier efficiency is approximately proportional to $Z/M^{1/2}$ [16], where Z is the charge and M is the mass of the ion. This factor needs to be taken into account since we are comparing ions with different charges and masses. This digital counting system ensures linearity over a very large dynamic range. The gas pressure is adjusted for different intensity ranges to keep the signal between 10^{-5} and 10^{-1} counts/shot.

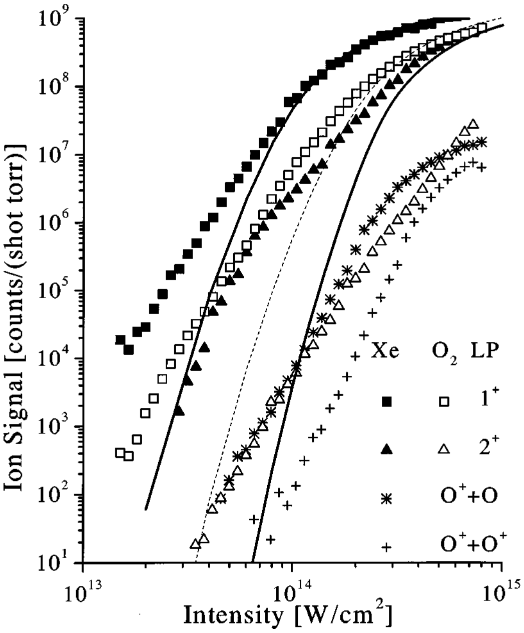

FIG. 2. Single- and double ionization yields for O_2 and Xe using linear polarization (LP). The full curves are the calculations based on the ADK model using single and double ionization potentials of Xe. The dashed curve fitting the $O_2{}^+$ data uses an ionization potential of 15 eV.

Absolute calibrations of both the laser intensity and the overall detection efficiency are needed to draw important conclusions from the data. The intensity was calibrated by fitting the Ar^+ LP ion yield to the ADK model. The rate was integrated over the measured pulse duration and focal volume. The adjustable parameters in the fit are the beam waist, detection efficiency, and extraction pinhole diameter, which controls the spatial volume sampled. The absolute detection efficiency was independently measured to be 0.5–1 % using correlation techniques. In this measurement, by monitoring one ion from a known molecular fragmentation pair, the probability of detecting the other ion gives a direct measurement of the overall detection efficiency. The fitted detection efficiency agrees with this measured value within a factor of 2. The absolute intensity based on fitting the Ar^+ ion yield agreed with the intensity calculated from the measured beam-spot size, pulse duration, and energy also to within a factor of 2. All of the other ADK curves (Figs. 1–3) use the experimental parameters determined from the Ar^+ LP data. As can be seen, the agreement for the Ar, Xe, and N_2 data is excellent, except, of course, for the NSDI components. Because of the extraction pinhole, the volume saturation does not follow the usual $I^{3/2}$ dependency and approaches the intensity-selection-scanning limit [17]. One final experimental detail concerns the possible contamination of the $O_2{}^{2+}$ signal with thermal O^+ ions (ions from O_2 molecular fragmentation are well separated in TOF). Indeed, a small thermal O^{2+} signal is seen at the highest intensity and gives an indication of the thermal O^+ contamination. However, the

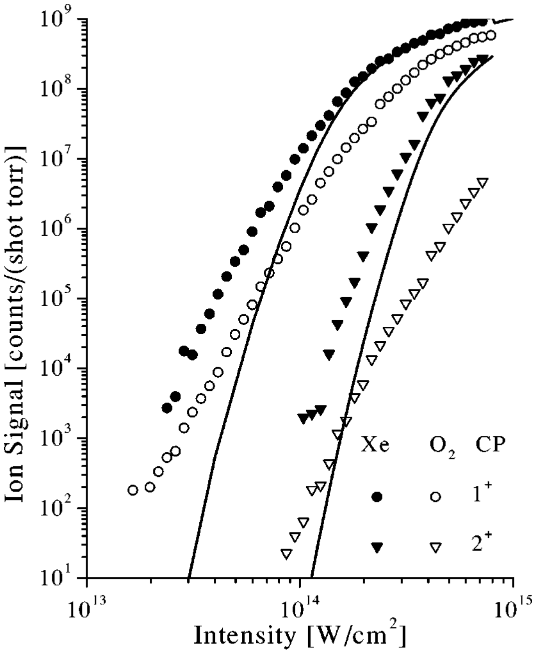

FIG. 3. Single- and double ionization yields for O_2 and Xe using circular polarization (CP). The full curves are the calculations based on the ADK model using single and double ionization potentials of Xe.

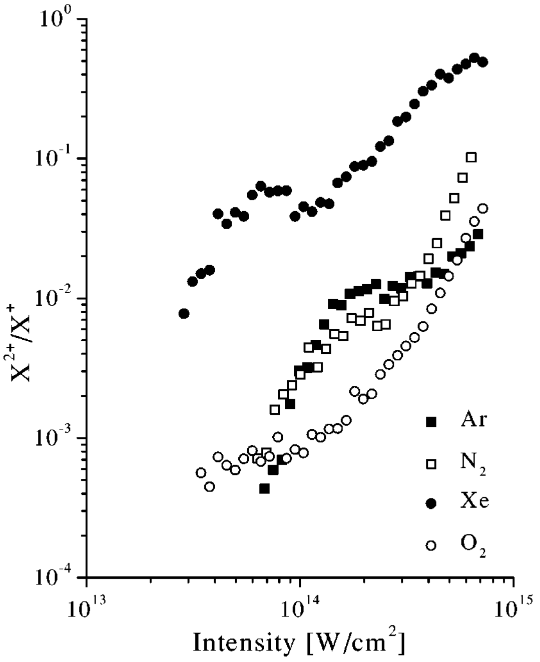

FIG. 4. Ratio curves of double/single ion yields are shown for N_2, Ar, O_2, and Xe using linear polarization (LP).

O^{2+} signal is completely independent of the O_2 pressure and thus only comes from background gases, presumably H_2O. Since the same must hold true for O^+, we could directly measure the O^+ contamination over the entire intensity range with just the base pressure in the vacuum chamber. Its influence on the data is negligible.

The ion yields of $N_2{}^+$ and $N_2{}^{2+}$ are very similar to Ar^+ and Ar^{2+} for both LP and CP over the entire intensity range (Fig. 1), as would be expected from a tunneling model depending only on I_p. However, we must also consider the dissociation channels of the molecule. For single ionization, the dissociation of $N_2{}^+$ is found to be quite small and, thus, does not influence the $N_2{}^+$ ion yield. Dissociation is more significant for double ionization because the $N^+ + N^+$ signal is comparable to the metastable $N_2{}^{2+}$ signal. However, these two signals have the same intensity dependence, in agreement with Ref. [18], which implies that both $N_2{}^{2+}$ and $N^+ + N^+$ originate from the same molecular complex, and that the ionization dynamics are the same for both dissociating and metastable states, including NSDI. To be sensitive to possible anomalies in NSDI we must be careful to choose a model-free definition. Many properties could be used as a signature of NSDI but most of them are based on a certain model. An ellipticity dependence assumes that either NSDI is due to rescattering or has restrictive angular-momentum selection rules [5]. Fitting the ''knee'' structure with a constant ratio of the single tunneling-ionization rate assumes that NSDI is due to a tunneling process [5,7]. However, the intensity dependence of the ratio X^{2+}/X^+ has been used to indicate NSDI [5], where X^+ and X^{2+} are the yields for single and double ionization of some atom or molecule X. Nonsequential dynamics are most fundamentally related to this ratio; if this ratio is only weakly dependent on intensity, it shows that the precursor to X^{2+} is not X^+. In Fig. 4, the ratios of N_2 and Ar approach the sequential ion yield of X^{2+} when the average intensity is higher than 3×10^{14} W/cm^2 and X^+ has saturated. The weak dependence of the ratio on intensity in the range of 1.2×10^{14} W/cm^2 to 3×10^{14} W/cm^2 reflects the nonsequential aspect of double ionization. Finally, the ratios fall at an intensity below 1.2×10^{14} W/cm^2, where the multiphoton effects in X^+ become significant. The rates for NSDI of N_2 and Ar are quite similar. The overall similarity of single and double ionization between N_2 and Ar indicates that the N_2 tunnel ionizes as if it were a structureless atom. Furthermore, the dissociation channels open to $N_2{}^+$ and $N_2{}^{2+}$ do not appear to play a significant role in strong-field ionization.

In agreement with the previous experiments mentioned above, Fig. 2 shows that the $O_2{}^+$ LP ion yield is roughly ten times below Xe^+ in the unsaturated range of the data. The LP and CP data of Xe^+ fit the ADK model very well, implying that the discrepancy between the $O_2{}^+$ and Xe^+ ion yields is not due to the enhancement of Xe^+ production, but truly a suppression of the $O_2{}^+$ data. We consider five different possible reasons for this observation covering a wide range of effects such as dissociative recombination, other dissociative processes, the Stark shift of the ground state, accidental resonances, and electron localization:

(1) Dissociative recombination through rescattering has been proposed to explain the suppression of the $O_2{}^+$ signal [11] as discussed above. However, all rescattering phenomena must exhibit a strong ellipticity dependence because in CP laser light, the probability for the ionized electron returning to the ion core will be vanishingly small [19]. As we now show in Fig. 3, the suppression of the $O_2{}^+$ signal persists with CP, ruling out DR as the major mechanism.

(2) Other dissociation mechanisms must also be considered. If $O_2{}^+$ dissociates into O^+ and O then, as above, the $O_2{}^+$ signal would be reduced. However, as seen in Fig. 2, the O^+ signal is far too small to account for the suppression of $O_2{}^+$. Even assuming O_2 could dissociate through some process that does not have a strong ellipticity dependence, the volume saturation of the $O_2{}^+$ data implies that all of the available O_2 are ionized to $O_2{}^+$ and detected as such. This rules out any dissociate process in the saturated region and we consider it unlikely that dissociation plays a significant role even at low intensities.

(3) Molecular polarizabilities α are generally larger than atomic ones. Polarizability leads to a lowering of the energy of the ground state through the Stark shift for any frequency below the first resonance. The Stark shift will increase the ionization potential of atoms and molecules, making them harder to be ionized. However, α_{Xe} (4.04×10^{-24} cm^3) is much larger than α_{O_2} (1.58×10^{-24} cm^3), which would make Xe harder to be ionized than O_2 if this is even a significant factor.

(4) The presence of any accidental electronic resonance in the molecule will enhance the $O_2{}^+$ yield rather than suppress it.

(5) Electron localization in diatomic molecules at a critical internuclear separation has been seen to greatly increase ionization rates [20] but, again, not to decrease them.

Thus, in considering general differences between atoms and molecules, we have found no effect that can explain the suppression of the $O_2{}^+$ signal. In order to characterize the anomaly, we find that the $O_2{}^+$ ion yield can be fit reasonably well to an ADK rate if we use an ionization potential of 15 eV. We note that this ionization potential falls between the two ionization limits of O_2, leading to the *X* and *A* state of ${O_2}^+$, 12.06 and 16 eV, respectively.

Xe has the lowest second ionization potential of all of the four gases that we studied and thus we cannot make a quantitative comparison between Xe^{2+} and ${O_2}^{2+}$. However, the double-ionization yield of Xe looks qualitatively like N_2 and Ar, although the NSDI rate is about five times higher (Fig. 4). Using circular polarization, Xe^{2+} falls off rapidly at an intensity below 1×10^{14} W/cm^2, and shows the ellipticity dependency seen in NSDI [5]. Unlike all the other species mentioned above, ${O_2}^+$ and ${O_2}^{2+}$ ion yields remain relatively parallel over the whole intensity range, resulting in an unusual intensity dependence of the ratio ${O_2}^{2+}/{O_2}^+$. On the one hand, Fig. 4 shows that O_2 exhibits NSDI but with a rate much lower than the other three gases. On the other hand, the ratio curve of ${O_2}^{2+}/{O_2}^+$ does not drop at low intensity. To our knowledge, this is the first documentation of an anomaly in the double ionization of O_2. Like N_2, the $O^+ + O^+$ signal is comparable to the ${O_2}^{2+}$ signal. However, the intensity dependence of the signals is noticeably different. This implies that the dissociating states are distinct from the metastable states and have different ionization dynamics. This difference requires further investigation, but the $O^+ + O^+$ signal appears to have an even smaller NSDI component.

In summary, we have compared the single and double ionization of two molecules N_2 and O_2. Both singly and doubly ionized N_2 behave like a structureless atom. The ${O_2}^+$ ion yield is below the tunneling rate, but this is not due to dissociation. Furthermore, we find significantly different intensity dependences of the ion yields for the metastable and dissociating states of doubly ionized O_2, and both have anomalously low NSDI rates. Therefore, the nonatomiclike behavior of O_2 appears to be due to the more complicated electronic structure. It should be noticed that N_2 has a closed-shell electronic structure, while the outermost orbital $(1\pi_g)^2$ of the ground-state O_2 is only half-filled and in a triplet state. It seems quite reasonable to expect that a closed-shell molecule will behave like a rare-gas atom, but not a molecule with an open-shell structure.

We would like to acknowledge support from the NSF under Grant No. PHY-9502935. G. N. Gibson was also supported through funding from the Research Corporation.

[1] P. Agostini *et al.*, Phys. Rev. Lett. **42**, 1127 (1979).
[2] A. McPherson *et al.*, J. Opt. Soc. Am. B **4**, 595 (1987); M. Bellini *et al.*, Phys. Rev. Lett. **81**, 297 (1998).
[3] D. N. Fittinghoff *et al.*, Phys. Rev. Lett. **69**, 2642 (1992).
[4] K. Kondo *et al.*, Phys. Rev. A **48**, R2531 (1993).
[5] B. Walker *et al.*, Phys. Rev. Lett. **73**, 1227 (1994).
[6] M. V. Ammosov *et al.*, Z. Eksp. Teor. Fiz. **91**, 2008 (1986) [Sov. Phys. JETP **64**, 1191 (1986)].
[7] A. Talebpour *et al.*, J. Phys. B **30**, 1721 (1997).
[8] G. Gibson *et al.*, Phys. Rev. A **41**, 5049 (1990).
[9] G. N. Gibson *et al.*, Phys. Rev. Lett. **67**, 1230 (1991).
[10] S. L. Chin *et al.*, J. Phys. B **25**, L249 (1992); T. D. G. Walsh *et al.*, *ibid.* **26**, L85 (1993); **27**, 3767 (1994).
[11] A. Talebpour *et al.*, J. Phys. B **29**, L677 (1996).
[12] C. W. Siders *et al.*, in *Ultrafast Phenomena XI*, edited by W. Zinth and J. G. Fujimoto (Springer-Verlag, Berlin, in press).
[13] M. Li and G. N. Gibson, J. Opt. Soc. Am. B **15**, 2404 (1998).
[14] G. N. Gibson *et al.*, Phys. Rev. Lett. **79**, 2022 (1997).
[15] W. C. Wiley and I. H. McLaren, Rev. Sci. Instrum. **26**, 1150 (1955).
[16] C. Cornaggia *et al.*, Phys. Rev. A **44**, 4499 (1991).
[17] P. Hansch and L. D. Van Woerkom, Opt. Lett. **21**, 1286 (1996).
[18] C. Cornaggia and Ph. Hering, J. Phys. B **31**, L503 (1998).
[19] P. B. Corkum, Phys. Rev. Lett. **71**, 1994 (1993); M. Protopapas *et al.*, *ibid.* **79**, 4550 (1997).
[20] T. Seideman *et al.*, Phys. Rev. Lett. **75**, 2819 (1995).